Available online at www.sciencedirect.com
SCIENCE DIRECT®
Journal of Organometallic Chemistry 691 (2006) 2228–2236
Journal of Organometallic Chemistry
www.elsevier.com/locate/jorganchem

Expression of chirality in salicyloxazolinate complexes of zirconium

Ian Westmoreland [1], Ian J. Munslow, Adam J. Clarke, Guy Clarkson, Robert J. Deeth, Peter Scott *

Department of Chemistry, University of Warwick, Gibbett Hill Road, Coventry CV4 7AL, UK

Received 12 October 2005; received in revised form 30 October 2005; accepted 30 October 2005
Available online 9 December 2005

Abstract

Treatment of chiral non-racemic salicyloxazoline proligands H**L** with tetrabenzylzirconium(IV) gave species [$\mathbf{L}_2Zr(CH_2Ph)_2$]. Reactions of K**L** with $ZrCl_4(THF)_2$ gave similar chloro complexes. One example of a benzyl complex was shown to exist as the Λ-*trans*,*cis*,*cis* diastereomer by X-ray crystallography. DFT calculations showed the observed isomer to be the most stable by 35 kJ mol^{-1}, indicating that thermodynamic diastereoselection for this species is excellent. Examination of the chiral environment about the benzyl co-ligands indicates however that the degree of expression of the chirality of the structure in what would be the site of metal-based reactions is poor in comparison to related systems. Variable temperature ^{1}H NMR data are consistent with this in that the low temperature spectrum exhibits a very small chemical shift difference between the chemically inequivalent benzylic C*H* atoms, and at higher temperatures dissociation of the portion of the ligand that contains the chiral information, i.e., the oxazoline unit, leads to apparent equivalence.

Keywords: Zirconium; Oxazoline; Diastereoselection; Fluxionality

1. Introduction

Octahedral coordination complexes may contain an element of chirality by virtue of an enantiomeric arrangement of, for example, three bidentate ligands about the metal [1,2]. Using chiral nonracemic ligands, one enantiomer may be formed preferentially as a result of kinetic or thermodynamic diastereoselection [3–7]. The situation is complicated by the great structural variety possible in organometallic and coordination compounds and also the range in kinetic stabilities of coordination environments. Accordingly, most studies on chiral metal complexes have involved later transition elements where d-orbitals tend to control the structure of the inner coordination sphere and the rates of topographical exchange are generally slow enough to be studied on convenient experimental timescales. For the early transition metals and f elements, where bonds are principally electrostatic and the rates of exchange are greater, very high levels of thermodynamic discrimination are probably needed in order to make systems that are of practical value.

The problem is deepened by the need for free or potentially free coordination sites where useful reactions might take place [6]. The synthesis of single diastereomeric chiral-at-metal complexes for which this criterion is satisfied has been achieved hitherto through the use of multidentate ligands, although the design and synthesis of such coordination environments also presents synthetic challenges [8]. Bidentate ligands are more readily available and more diverse in nature than multidentate systems, and if the aim is to produce chiral metal catalysts then, for e.g. group 4 metals, this points us toward octahedral complexes of the type $[M(AB)_2X_2]$, where AB is a chiral bidentate monoanionic ligand. While this class of complex can in principle form eight diastereomers we have shown that it is quite possible to design highly diastereoselective systems for zirconium using the bidentate N–N ligands aminopyridinate[9,10] and aminooxazolinate [11]. Surprisingly high kinetic stability and excellent diastereoselection was found

* Corresponding author.
E-mail address: peter.scott@warwick.ac.uk (P. Scott).
[1] Present address: College of Chemistry, University of California at Berkeley, Berkeley, CA 94720-1460, USA.

0022-328X/$ - see front matter © 2005 Elsevier B.V. All rights reserved.
doi:10.1016/j.jorganchem.2005.10.055

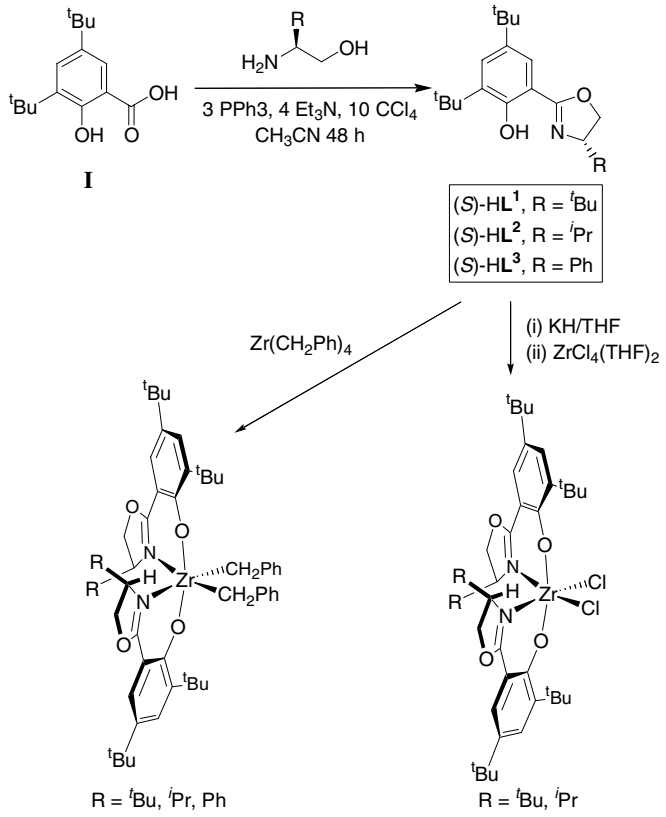

Scheme 1. Synthesis of bidentate proligands.

for a pyridine/alcoholate N–O system [12]. Another N–O ligand system, the salicyloxazolines (such as $\mathbf{L}^n$, Scheme 1), has been used to create chiral-at-metal complexes of later transition metals, particularly ruthenium [13]. Some group 4 metal complexes have been reported also, but the issue of diastereoselection in these compounds was not addressed [14]. We report here a range of complexes of salicyloxazolinates with zirconium, and a combined structural, computational and NMR spectroscopic study in respect of the stereogenic element at the metal.

2. Results and discussion

2.1. Proligand synthesis

The preparations of (*S*)-H$\mathbf{L}^{1-3}$ were accomplished in ca. 70% yield via reaction of 3,5-di-*tert*-butylsalicylic acid **I** with the appropriate amino alcohol after the method of Vorbruggen and Krolikiewicz [15,16] (Scheme 1). Treatment of the starting materials with triphenylphosphine, carbon tetrachloride and a base was found to be most effective using the quantities of these reagents as detailed in Scheme 1. Optimal conditions for this type of synthesis appear to be highly substrate dependant [17]. In order to maintain low concentrations of the chlorophosphonium salt and thus prevent side reactions, either the CCl_4 or PPh_3 is added to the reaction mixture over 4 h; it generally being more convenient to administer CCl_4 via syringe pump [18]. Our best results were obtained when the mixture was stirred for 48 h following completion of this addition. We also found that reaction performance was improved dramatically under anhydrous conditions; the pre-drying of commercial **I** being particularly beneficial. Experimentation with different solvents tended to favour acetonitrile over dichloromethane, while the effect of adding pyridine to the reaction mixtures as described by Vorbruggen was not studied [16a]. We further investigated reports by Sigman and Rajaram [18] that di-*iso*-propylethylamine can provide results preferential to those obtained with triethylamine, but were unable to discern any difference in this system.

2.2. Synthesis of complexes

Treatment of the potentially bidentate proligand (*S*)-H$\mathbf{L}^{1}$ with slightly less than half an equivalent of tetrabenzylzirconium(IV) in toluene at −78 °C gave an orange solution. Isolation of the crude material by drying in vacuo followed by recrystallisation from pentane at −35 °C gave the species [$\mathbf{L}^{1}_2$Zr$(CH_2Ph)_2$] as yellow microcrystals in 92% yield (Scheme 1). The isopropyl-substituted (*S*)-H$\mathbf{L}^{2}$ was treated with $Zr(CH_2Ph)_4$ at −78 °C in a similar manner. The single organometallic product of this reaction [$\mathbf{L}^{2}_2$Zr$(CH_2Ph)_2$] was isolated as an orange solid in 79% yield after recrystallisation from pentane. Reaction of two equivalents the phenyl-substituted proligand (*S*)-H$\mathbf{L}^{3}$ with $Zr(CH_2Ph)_4$ was less straightforward. Initial NMR-scale experiments at ambient temperature appeared to show the formation of mixtures of [$\mathbf{L}^{3}$Zr$(CH_2Ph)_3$] and [$\mathbf{L}^{3}_2$Zr$(CH_2Ph)_2$], although the latter was the major product. The slow addition of a solution of $Zr(CH_2Ph)_4$ to slightly more than two equivalents of H$\mathbf{L}^{3}$ at −78 °C in toluene was more successful. Recrystallisation from pentane of crude material thus obtained gave [$\mathbf{L}^{3}_2$Zr$(CH_2Ph)_2$] as an orange microcrystalline solid in 83% yield.

Treatment of the proligands (*S*)-H$\mathbf{L}^{1-3}$ with potassium hydride in THF provided the salts (*S*)-K$\mathbf{L}^{1-3}\cdot(\mathrm{THF})_n$. These compounds were isolated as white or pale yellow solids and the value of *n* was calculated from integration of the relevant ^{1}H NMR resonances from spectra recorded in d_5-pyridine. The isolation of these compounds is not a necessary step prior to salt metathesis with $ZrCl_4(THF)_2$, it usually being more convenient to carry out the latter reaction in situ.

Salt metathesis of $ZrCl_4(THF)_2$ with prepared (*S*)-K$\mathbf{L}^{1}\cdot(\mathrm{THF})n$ was straightforward, and resulted in the formation of a yellow product. Sublimation of this material at 260 °C, 10^{-6} mmHg, gave a pale yellow microcrystalline solid, which was shown to be [$\mathbf{L}^{1}_2$ZrCl_2]. The salt metathesis reaction of $ZrCl_4(THF)_2$ with (*S*)-K$\mathbf{L}^{2}\cdot(\mathrm{THF})n$ was rather capricious. Ultimately however, the treatment of an in situ prepared solution of (*S*)-K$\mathbf{L}^{2}$ with $ZrCl_4$(THF) at 0 °C did lead to the isolation of a pale yellow solid. Sublimation of this material at 265 °C/10^{-6} mmHg gave a pale yellow microcrystalline solid. Analysis of the sublimated compound confirmed the molecular formula as [$\mathbf{L}^{2}_2$ZrCl_2]. Although a

variety of reaction conditions were tested we were unable to develop a synthesis of adequately pure $[\mathbf{L}^{\mathbf{3}}_2ZrCl_2]$.

2.3. Molecular structure of $[\mathbf{L}^{\mathbf{1}}_2Zr(CH_2Ph)_2]$

Single crystals of $[\mathbf{L}^{\mathbf{1}}_2Zr(CH_2Ph)_2]$ suitable for X-ray structural determination were obtained by cooling a concentrated solution in pentane to −30 °C. In the solid state, the Λ-*trans*,*cis*,*cis* diastereomer is observed exclusively (Figs. 1 and 2(a)).

The complex is essentially C_2-symmetric with a six-coordinate zirconium centre at which the benzyl coligands occupy mutually *cis* positions. The geometry at the metal is distorted from octahedral due to the N–Z–O ligand bite angle for the six-membered chelates of ca. 77° (Table 1). The ligand nitrogen donor atoms also take up mutually *cis* coordination sites at the metal centre, the N–Zr–N bond angle being 99.1(3)°. Each nitrogen atom is *trans* to a benzyl ligand. The remaining mutually *trans* sites are occupied by the aryl oxygens at a O–Zr–O bond angle of 167.1(3). These and other metrical parameters are comparable to related Schiff base [19,20] and oxazoline [14] complexes.

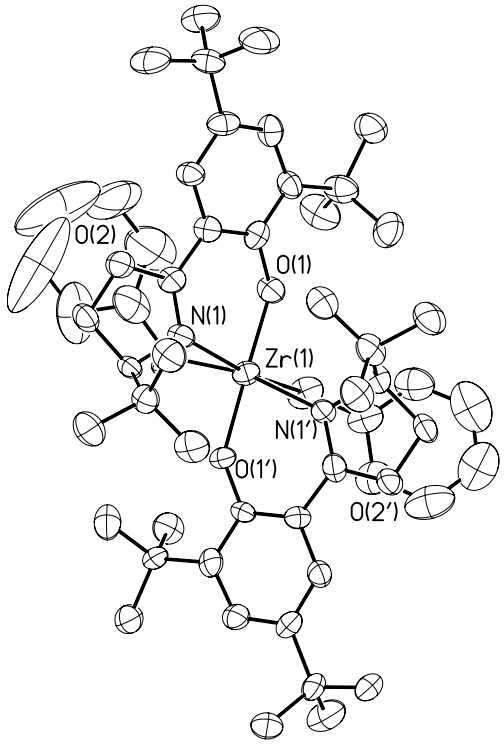

Fig. 1. Molecular structure of $[\mathbf{L}^{\mathbf{1}}_2Zr(CH_2Ph)_2]$ viewed along the crystallographic C_2 axis with benzyl ligands at the rear.

2.4. Computational investigation of the structure of $[\mathbf{L}^{\mathbf{1}}_2Zr(CH_2Ph)_2]$

We set out to investigate the relative energies of the six-coordinate diastereomers of $[\mathbf{L}^{\mathbf{1}}_2Zr(CH_2Ph)_2]$ via DFT [21]; predicted diastereoselectivities from this approach consis-

Table 1
Selected bond lengths (Å) and angles (°) for $[\mathbf{L}^{\mathbf{1}}_2Zr(CH_2Ph)_2]$

Zr(1)–O(1)	1.981(5)
Zr(1)–O(1′)	2.010(5)
Zr(1)–C(100)	2.319(11)
Zr(1)–C(200)	2.319(12)
Zr(1)–N(1)	2.403(7)
Zr(1)–N(1′)	2.417(8)
O(1)–Zr(1)–O(1′)	167.1(3)
O(1)–Zr(1)–C(100)	94.6(3)
O(1′)–Zr(1)–C(100)	95.1(3)
O(1)–Zr(1)–C(200)	97.0(4)
O(1′)–Zr(1)–C(200)	91.9(4)
C(100)–Zr(1)–C(200)	87.3(5)
O(1)–Zr(1)–N(1)	77.5(2)
O(1′)–Zr(1)–N(1)	94.0(2)
C(100)–Zr(1)–N(1)	168.8(3)
C(200)–Zr(1)–N(1)	85.9(4)
O(1)–Zr(1)–N(1′)	95.2(3)
O(1′)–Zr(1)–N(1′)	76.4(3)
C(100)–Zr(1)–N(1′)	89.3(4)
C(200)–Zr(1)–N(1′)	167.5(3)
N(1)–Zr(1)–N(1′)	99.1(3)
C(13)–O(1)–Zr(1)	146.4(6)
C(13′)–O(1′)–Zr(1)	143.2(7)

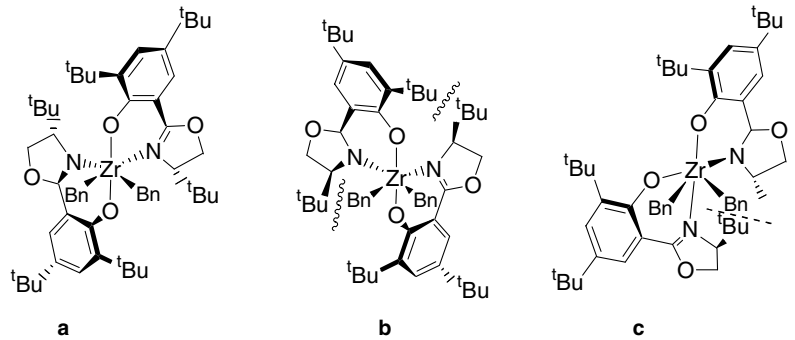

Fig. 2. Selected diastereomers of $[\mathbf{L}^{\mathbf{1}}_2Zr(CH_2Ph)_2]$: (a) Λ-*trans*,*cis*,*cis* observed in solid state rel. energy = 0 kJ mol^{-1}, (b) Λ-*trans*,*cis*,*cis* overlap of groups indicated, (c) Λ-*cis*,*cis*,*cis* rel. energy = 35 kJ mol^{-1}.

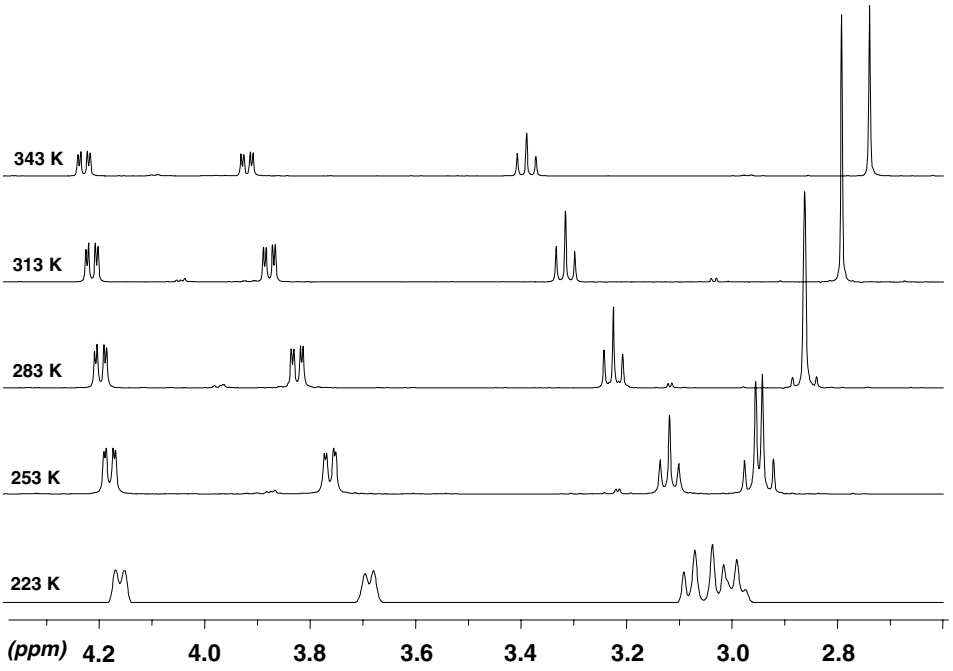

Fig. 3. Variable temperature ^{1}H NMR spectra of $[\mathbf{L}^1_2Zr(CH_2Ph)_2]$.

tently agree well with experimental observations in related systems [10–12].

Starting from the observed molecular structure of $[\mathbf{L}^1_2Zr(CH_2Ph)_2]$ we attempted to construct models of the remaining seven possible six-coordinate diastereomers using the MM2 package of Chem3D and standard bond lengths. In most cases these structures were found to be infeasible for steric reasons. For example, compare the observed Λ-*trans*,*cis*,*cis* diastereomer (Fig. 2(a)) with its partner of Δ helicity (b). In the Λ isomer, the oxazoline *tert*-butyl groups point into sterically unencumbered regions at the back of the complex as drawn, while for the inaccessible Δ isomer, these groups would necessarily be oriented towards the front, and *overlap* (rather than merely interact sterically) with the phenoxy *tert*-butyl substituents on neighbouring salicyloxazoline ligand. The only feasible alternative diastereomer was Λ-*cis*-*cis*-*cis* (c). This structure and the crystallographically observed Λ-*trans*, *cis*,*cis* isomer were investigated using DFT calculations. The minimised structure of the Λ-*cis*,*trans*,*cis* isomer (a) was essentially superimposable on that observed in the solid state. The Δ-*cis*,*cis*,*cis* diastereomer (c) was found to be 35 kJ mol^{-1} less stable; the most obvious unfavourable steric interaction, that between an oxazoline *tert*-butyl group and benzyl CH_2 is indicated in Fig. 2. In any event, we expect to observe only the Λ-*trans*,*cis*,*cis* isomer (a) in the gas phase.

2.5. NMR spectroscopic investigations

The complex $[\mathbf{L}^1_2Zr(CH_2Ph)_2]$ contains three stereogenic centres, two at C and one at Zr. No matter what the mechanism of epimerisation at the stereogenic Zr atom, so long as the ligands do not become detached, the benzyl methylene groups remain diastereotopic and would be expected to give rise to a pair of AB doublets in the ^{1}H NMR spectrum. It is not easy to quantify the effect of the presence of the asymmetry on the magnitude of the apparent chemical shift difference between H_A and H_B, i.e., how well the chirality of the system is expressed in this physical property [22]. Experience dictates however that in a given chiral-at-metal system with diastereotopic co-ligands, the magnitude of the splitting ($\Delta\delta$ ppm) is affected strongly by the degree of fluxionality; as temperature is increased and exchange processes become more rapid, $\Delta\delta$ tends to fall [9,10,12].

Fig. 3 shows portions of the ^{1}H NMR spectra of $[\mathbf{L}^1_2Zr(CH_2Ph)_2]$ recorded in d_8-toluene at various temperatures. At 343 K the oxazoline CH_2 proton *trans* to the C*H* hydrogen appears as an AB doublet at δ 4.23 ppm. The other CH_2 proton appears as a triplet at δ 3.40 ppm, and shows a vicinal coupling of 8 Hz to the C*H*, to which it is also *cis*. The low chemical shift of this signal can be explained by reference to the crystal structure (Fig. 1); the hydrogen from which it arises sits directly above the phenyl group of the Zr-benzyl, the shift to high field being a result of ring current. The second AB doublet at 3.92 is attributed to the C*H* itself, which also shows a coupling of 8 Hz to the two vicinal protons, but has a dihedral angle of about 90° with that to which it is *trans* resulting in the observed fine splitting. The zirconium-bound benzyl CH_2 protons, despite being chemically inequivalent (vide supra), give rise to a singlet resonance observed at δ 2.73 ppm.[2] A

[2] In dichloromethane-d^2 at ambient temperature the Zr–CH_2 groups give rise to a pair of AB doublets with apparent $\Delta\delta$ of only 0.05 ppm.

very small amount of a minor species, most likely an impurity, though possibly also a different isomer, is observed at δ 2.97 and 4.08 ppm. Cooling of the sample leads to changes in the chemical shift for all of these resonances. By 253 K the chemical shifts of the benzyl CH_2 protons are sufficiently different that the expected second order pair of AB doublets is observed (ca. δ 2.93 ppm). Conversely, the oxazoline CH_2 proton resonates at lower frequency as the temperature is decreased, although by 253 K there is little discernable change in the shape of signal. By 223 K the resonances for these protons overlap, but $\Delta\delta$ for the benzyl CH_2 group has risen to ca. 0.06 ppm. Much below this temperature, increased viscosity of the solvent causes extreme broadening. The complexes $[\mathbf{L}^{n}_{2}\mathrm{Zr}(\mathrm{CH_2Ph})_2]$ ($\boldsymbol{n} = \mathbf{2},\mathbf{3}$), and indeed $[\mathbf{L}^{n}_{2}\mathrm{ZrCl_2}]$ ($\boldsymbol{n} = \mathbf{1},\mathbf{2}$) behave in a very similar manner.

The DFT calculations detailed above predict the existence of a single diastereomer for this compound. It is evident however that the system is undergoing structural change down to 223 K and perhaps lower on the NMR chemical shift timescale at that temperature, presumably between the six-coordinate Λ-*trans*,*cis*,*cis* isomer and unobserved five-coordinate species via *N*-dissociation. The appearance of the spectra as temperature is increased is consistent with this; the reduction in $\Delta\delta$ for the Zr–CH_2 signals probably arises as a result of the increased average distance between these units and the stereogenic centres on the oxazoline ligands, and simultaneously poorer expression of chirality at metal. This behaviour contrasts with that displayed by $[(\mathrm{NO^*})_2\mathrm{Zr}(\mathrm{CH_2Ph})_2]$ (Fig. 4) using the same solvent and magnetic field strength [12]. This system is clearly in the slow exchange regime below 273 K showing only one diastereomer ($\Delta\delta$ for benzyl $\mathrm{CH_AB_B}$ doublets ca. 0.3 ppm). On increasing the temperature, the signals for H_A and H_B broaden but do not coalesce, then finally resharpen at new chemical shifts in the fast exchange regime above 353 K. Notably *N*-dissociation in this system does not increase the distance of the stereogenic C centres from the inner coordination sphere. A similar comparison is possible between the present system and our recently reported chiral aminopyridinates [10] where the portion of the ligand remaining bonded to the metal contains the chiral information.

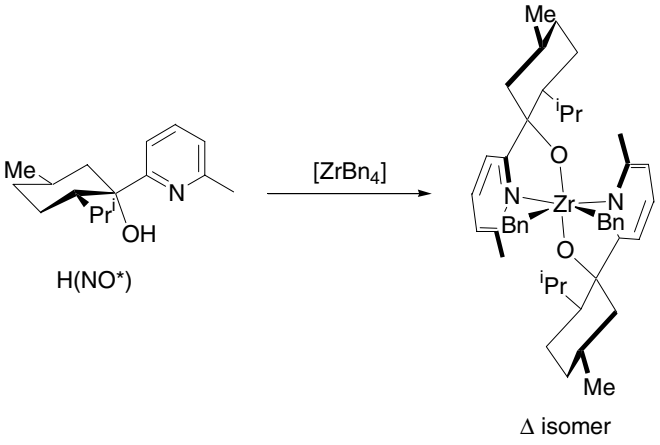

Fig. 4. A pyrdininealcoholate complex of zirconium, $[(\mathrm{NO^*})_2\mathrm{Zr}(\mathrm{CH_2Ph})_2]$ [12].

A space-filling model of the computed structure of Λ-*trans*, *cis*, *cis*-$[\mathbf{L}^{1}_{2}\mathrm{Zr}(\mathrm{CH_2Ph})_2]$ is shown in Fig. 5(a), with approximately the same orientation as that shown in Fig. 2(a) (i.e., viewed along the C_2-axis with the two CH_2Ph groups toward the front). The analogous structure of Δ-*trans*,*cis*,*cis*-$[(\mathrm{NO^*})_2\mathrm{Zr}(\mathrm{CH_2Ph})_2]$ is shown for comparison [12]. For the $\mathbf{L^1}$ complex, the benzyl H atoms are in rather similar environments. For the NO* complex the chirality of the system is expressed very strongly, leading to an S-shaped conformation of the $Zr(CH_2Ph)_2$ units which places the H atoms in distinctly different environments.

3. Conclusion

The salicyloxazoline proligands (*S*)-H$\mathbf{L^{1–3}}$ give C_2-symmetric compounds of the form $[\mathbf{L^{1–3}}_{2}\mathrm{ZrX_2}]$. Examination

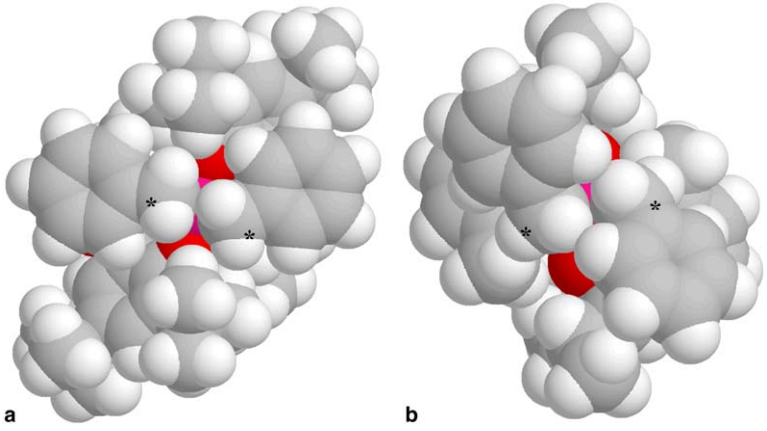

Fig. 5. Space-filling models of (a) Λ-*trans*, *cis*, *cis*-$[\mathbf{L}^{1}_{2}\mathrm{Zr}(\mathrm{CH_2Ph})_2]$ and (b) Δ-*trans*,*cis*,*cis*-$[(\mathrm{NO^*})_2\mathrm{Zr}(\mathrm{CH_2Ph})_2]$; benzyl C atoms marked with *.

of the solid state structure of $[\mathbf{L}^{\mathbf{1}}_2\mathrm{Zr}(\mathrm{CH_2Ph})_2]$, and DFT calculations on this and the only other feasible diastereomer point toward the existence of only one six-coordinate species at equilibrium. Nevertheless the degree of expression of the chirality of the structure in what would be the site of metal-based reactions is poor in comparison to other Zr systems, as assessed from the molecular structure and variable temperature ^{1}H NMR data.

4. Experimental

4.1. General details

Where necessary, procedures were carried out under an inert atmosphere of argon by using a dual manifold vacuum/argon line and standard Schlenk techniques, or in an MBraun dry box (<1 ppm O_2/H_2O). Solvents were dried by refluxing for three days under dinitrogen over the appropriate drying agents (sodium for toluene; potassium for THF, benzene and heptane; sodium–potassium alloy for diethyl ether, petroleum ether, and pentane; calcium hydride for carbon tetrachloride, dichloromethane, pyridine and acetonitrile) and were degassed before use. Solvents were stored in glass ampoules under argon. All glassware and cannulae and Celite were stored in an oven at >373 K. Deuterated solvents were freeze–thaw degassed and dried by refluxing over potassium (for benzene, toluene and THF) or calcium hydride (for dichloromethane, pyridine and acetonitrile) for three days before trap-to-trap distillation and storage in the dry box. Deuterated chloroform was dried in the bottle over molecular sieves (4 Å). Hydrated 3,5-di-*tert*-butylsalicylic acid was dried thoroughly and recrystalised prior to use. Triethylamine was dried by distillation from calcium hydride. Sodium hydride dispersion in mineral oil was placed in a Schlenk vessel under an inert atmosphere and washed three times with diethyl ether to remove the oil. The solid was subsequently dried thoroughly and stored in the dry box. All other purchased chemical reagents were used as received.

Flash chromatography was performed either in standard glassware or with a FlashMaster Personal chromatography system and a selection of pre-packed disposable columns. Thin-layer chromatography was performed using Merck 0.25 mm silica layer foil-backed plates.

NMR spectra were recorded on Bruker ACF-250, DPX-300, DPX-400, AV-400 and DPX-500 spectrometers. ^{1}H and ^{13}C spectra were referenced internally using residual protio solvent resonances relative to tetramethylsilane ($\delta = 0$ ppm). Proton and carbon NMR assignments were routinely confirmed by ^{1}H–^{1}H (COSY) or ^{1}H–^{13}C (HMQC) experiments. Infra-red spectra were obtained either as Nujol mulls using a Perkin–Elmer Paragon 1000 FTIR spectrometer, or directly using an Avatar 320 FTIR instrument. EI and CI mass spectra were obtained on a VG Autospec mass spectrometer. Elemental analyses were performed by Warwick Analytical Services.

4.2. Proligand synthesis

The following represents our refined general procedure for the synthesis of proligands $\mathbf{HL^{1-3}}$: Acetonitrile (50 ml) was added to a Schlenk vessel charged with 3,5-di-*tert*-butylsalicylic acid (2.0 g, 8.0 mmol), appropriate amino alcohol (8.0 mmol) and triphenylphosphine (6.30 g, 24.0 mmol). To the resulting white suspension was added triethylamine (4.5 ml, 32.0 mmol) with stirring, and a colourless solution was obtained after about 10 min. Carbon tetrachloride (7.8 ml, 80 mmol) was added dropwise to the reaction mixture over 4 h. During the course of the addition the solution became cloudy, and changed colour; first to yellow, then orange, and ultimately dark red, or even dark brown in some instances. The mixture was stirred for a further 48 h following completion of the addition. The solution was then filtered, and diethyl ether (30 ml) was added to the red filtrate. Shaking of this mixture resulted in the precipitation of a white solid which was also removed by filtration. The filtrate was concentrated in vacuo a leave a dark red residue. This material was extracted with hexane (100 ml) over 4 h. The extract was filtered, and concentrated under reduced pressure to yield an orange solid. This material was eluted through a column of silica gel using a hexane:ethyl acetate (20:1) mobile phase. Product containing fractions were identified by thin layer chromatography and collected. Removal of the solvent under reduced pressure gave the product as a white microcrystalline solid.

4.2.1. (*S*)-$\mathbf{HL^1}$

From (*S*)- *tert*-leucinol (936 mg, 8.0 mmol). Yield 1.91 g, 72%. ^{1}H NMR δ_H (400 MHz, 298 K, $CDCl_3$) 12.64 (1H, bs, O*H*), 7.44 (1H, d, $^4J_{HH} = 2$ Hz, Ar–*H*), 7.36 (1H, d, $^4J_{HH} = 2$ Hz, Ar–*H*), 4.24 (1H, dd, $^2J_{HH} = 9$ Hz, $^3J_{HH} = 2$ Hz, CH_2), 4.11 (1H, t, $^3J_{HH} = 8$ Hz, CH_2), 4.03 (1H, dd, $^2J_{HH} = 9$ Hz, $^3J_{HH} = 2$ Hz, C*H*), 1.37 (9H, s, ^{t}Bu) 1.23 (9H, s, ^{t}Bu) 0.88 (9H, s, ^{t}Bu) ppm.

^{13}C{^{1}H} NMR δ_C (100.6 MHz, 298 K, $CDCl_3$) 166.0, 157.1, 139.9, 136.4, 127.9, 122.1, (Ar), 109.8 (*C*=N), 75.1 (*C*H), 67.8 (*C*H_2), 35.2, 34.3, 33.8 (*C*Me_3), 31.5, 29.5, 25.9 (C *Me*$_3$) ppm.

MS (EI$^+$) *m*/*z*: 331 (100%, M^+), 316 (85%, M^+-CH_3), 274 (60%, $M^+-{}^t$Bu).

IR (Golden gate) ν cm^{-1}: 2961, 2906, 2867, 1633, 1596, 1437, 1392, 1368, 1362, 1287, 1254, 1219, 1204, 1189, 1106, 1028, 979, 892, 822, 784, 70, 727.

EA Calc. for $C_{21}H_{33}NO_2$: C, 76.09; H, 10.03; N, 4.23. Found: C, 76.29; H, 10.11; N, 4.17%.

4.2.2. (*S*)-$\mathbf{HL^2}$

From (*S*)-(+)-2-amino-3-methyl-1-butanol (825 mg, 8.0 mmol). Yield 1.7 g, 67%. ^{1}H NMR δ_H (400 MHz, 298 K, $CDCl_3$) 12.63 (1H, bs, O*H*), 7.45 (1H, d, $^4J_{HH} = 2$ Hz, Ar–*H*), 7.36 (1H, d, $^4J_{HH} = 2$ Hz, Ar–*H*), 4.32 (1H, m, CH_2), 4.06 (2H, m, CH_2 and C*H*), 1.78 (1H,

m, C*H*Me$_2$), 1.37 (9H, s, ^{t}Bu) 1.28 (9H, s, ^{t}Bu), 0.96 (3H, s, *Me*), 0.88 (3H, s, *Me*) ppm.

^{13}C{^{1}H} NMR δ_C (100.6 MHz, 298 K, $CDCl_3$) 166.0, 157.0, 139.9, 136.4, 127.9, 122.1 (Ar), 109.8, (*C*=N), 71.7 (*C*H), 69.6 (*C*H$_2$), 35.2, 34.3, (*C*Me$_3$), 33.1, (*C*HMe$_2$), 31.5, 29.5 (C *Me*$_3$), 18.9, 18.7 (CH*Me*$_2$) ppm.

MS (EI$^+$) *m/z*: 317 (100%, M$^+$), 302 (85%, M$^+$−CH$_3$), 260 (45%, M$^+$−^{t}Bu).

IR (Golden gate) ν cm^{-1}: 2959, 2870, 1633, 1595, 1468, 1437, 1391, 1362, 1288, 1274, 1253, 1215, 1188, 1103, 1044, 1030, 980, 822, 783, 772, 765, 728.

EA Calc. for $C_{20}H_{31}NO_2$: C, 75.67; H, 9.84; N, 4.41. Found: C, 75.66; H, 9.87; N, 4.18%.

4.2.3. (*S*)-H**L**^{3}

From (*S*)-(+)-2-phenylglycinol (1.10 g, 8.0 mmol). Yield 2.1 g, 75%. ^{1}H NMR δ_H (400 MHz, 298 K, $CDCl_3$) 12.48 (1H, bs, O*H*), 7.56 (1H, d, $^4J_{HH} = 2$ Hz, Ar–*H*), 7.42 (1H, d, $^4J_{HH} = 2$ Hz, Ar–*H*), 7.31 (2H, m, Ar–*H*), 7.26 (3H, m, Ar–*H*), 5.40 (1H, dd, $^2J_{HH} = 8$ Hz, $^3J_{HH} = 2$ Hz, C*H*$_2$), 4.72 (1H, dd, $^2J_{HH} = 8$ Hz, $^3J_{HH} = 2$ Hz, C*H*), 4.18 (1H, t, $^3J_{HH} = 8$ Hz, C*H*$_2$), 1.40 (9H, s, ^{t}Bu) 1.28 (9H, s, ^{t}Bu) ppm.

^{13}C{^{1}H} NMR δ_C (100.6 MHz, 298 K, $CDCl_3$) 167.2, 157.1, 141.8, 140.1, 136.6, 128.8, 128.3, 127.8, 126.6, 122.3 (Ar), 109.6 (*C*=N), 73.8 (*C*H$_2$), 69.0 (*C*H), 35.2, 34.3 (*C*Me$_3$), 31.5, 29.5 (C *Me*$_3$) ppm.

MS (EI$^+$) *m/z*: 351 (100%, M$^+$), 336 (85%, M$^+$−CH$_3$), 294 (30%, M$^+$−^{t}Bu).

IR (Golden gate) ν cm^{-1}: 2958, 1632, 1439, 1390, 1367, 1344, 1276, 1252, 1187, 1141, 1103, 980, 894, 820, 786, 754, 717.

EA Calc. for $C_{23}H_{29}NO_2$: C, 78.59; H, 8.32; N, 3.99. Found: C, 78.50; H, 8.46; N, 3.95%.

4.3. Potassium salts of proligands

THF (15 ml) was added to a Schlenk vessel charged with proligand (0.55 mmol) and potassium hydride (44 mg, 1.10 mmol). The resulting yellow suspension was stirred for 15 h under reduced pressure. After this time the stirring was ceased and unreacted KH was allowed to settle. The solution was filtered via cannula, and the yellow filtrate was concentrated in vacuo to yield a yellow microcrystalline solid. Analysis by ^{1}H NMR spectroscopy in d_5-pyridine enabled the composition of the product to be established.

4.3.1. (*S*)-K**L**^{1} · (*THF*)$_{0.75}$

Yield 241 mg, 93%. ^{1}H NMR (400 MHz, 298 K, d_5-pyridine): δ_H 8.04 (1H, d, $^4J_{HH} = 3$ Hz, Ar–*H*), 7.61 (1H, d, $^4J_{HH} = 3$ Hz, Ar–*H*), 4.07 (3H, m, C*H* and C*H*$_2$), 3.67 (m, THF), 1.74 (9H, s, ^{t}Bu), 1.63 (m, THF), 1.45 (9H, s, ^{t}Bu), 0.88 (9H, s, ^{t}Bu).

4.3.2. (*S*)-K**L**^{2} · (*THF*)$_{1.25}$

Yield 260 mg, 93%. ^{1}H NMR (400 MHz, 298 K, d_5-pyridine): δ_H 8.07 (1H, d, $^4J_{HH} = 3$ Hz, Ar–*H*), 7.60 (1H, d, $^4J_{HH} = 3$ Hz, Ar–*H*), 4.15 (1H, m, C*H*$_2$), 3.95 (2H, m, C*H* and C*H*$_2$), 3.60 (m, THF), 1.85 (1H, m, C*H*Me$_2$), 1.74 (9H, s, ^{t}Bu), 1.60 (m, THF), 1.43 (9H, s, ^{t}Bu), 0.83 (3H, s, C*H*$_3$), 0.73 (3H, s, C*H*$_3$).

4.3.3. (*S*)-K**L**^{3} · (*THF*)$_{0.80}$

Yield 210 mg, 92%. ^{1}H NMR (400 MHz, 298 K, d_5-pyridine): δ_H 8.14 (1H, d, $^4J_{HH} = 3$ Hz, Ar–*H*), 7.66 (1H, d, $^4J_{HH} = 3$ Hz, Ar–*H*), 7.32 (2H, m, Ar–*H*), 7.17 (3H, m, Ar–*H*), 5.35 (1H, m, C*H*$_2$), 4.33 (1H, m, C*H*), 3.91 (1H, m, C*H*$_2$), 3.60 (m, THF), 1.79 (9H, s, ^{t}Bu), 1.60 (m, THF), 1.49 (9H, s, ^{t}Bu).

4.4. Zirconium benzyls

4.4.1. [**L**$_2^1$*Zr*(*CH*$_2$*Ph*)$_2$]

A solution of Zr(CH$_2$Ph)$_4$ (153 mg, 0.336 mmol) in toluene (10 ml) was cooled to −78 °C with stirring. To this was added a solution of (*S*)-H**L**^{1} (222 mg, 0.670 mmol) in toluene (10 ml). The resulting yellow solution was stirred at this temperature for 1 h in the absence of light. The cold bath was then removed and the reaction mixture was allowed to warm to ambient temperature. Stirring was continued for a further 15 h. After this time the solvent was removed in vacuo, and an orange residue was obtained. The residue was re-dissolved in pentane and filtered. The filtrate was reduced in volume to ca. 5 ml, and cooled to −30 °C. After cooling for 12 h at this temperature, the product was obtained as fine orange crystals. Yield 331 mg, 92%.

^{1}H NMR δ_H (400 MHz, 298 K, CD_2Cl_2) 7.54 (2H, d, $^4J_{HH} = 2$ Hz, Ar–*H*), 7.49 (2H, d, $^4J_{HH} = 2$ Hz, Ar–*H*), 6.66 (4H, t, $^3J_{HH} = 7$ Hz, Ar–*H*), 6.51 (4H, d, $^3J_{HH} = 7$ Hz, Ar–*H*), 6.40 (2H, d, $^3J_{HH} = 7$ Hz, Ar–*H*), 4.09 (2H, dd, $^2J_{HH} = 8$ Hz, $^3J_{HH} = 2$ Hz, oxazoline C*H*$_2$), 4.00 (2H, dd, $^2J_{HH} = 8$ Hz, $^3J_{HH} = 2$ Hz, oxazoline C*H*), 3.28 (2H, t, $^3J_{HH} = 8$ Hz, oxazoline C*H*$_2$), 2.25 (2H, d, $^2J_{HH} = 10$ Hz, benzyl C*H*$_2$), 2.20 (2H, d, $^2J_{HH} = 10$ Hz, benzyl C*H*$_2$), 1.61 (18H, s, ^{t}Bu) 1.26 (18H, s, ^{t}Bu), 0.50 (18H, s, ^{t}Bu) ppm.

^{13}C{^{1}H} NMR δ_C (100.6 MHz, 298 K, CD_2Cl_2) 172.8, 160.7, 151.8, 141.1, 138.0, 130.2, 127.8, 125.3, 124.5, 119.3 (Ar), 116.7 (*C*=N), 73.5, (*C*H), 69.3 (oxazoline *C*H$_2$), 67.9 (benzyl *C*H$_2$), 35.8, 35.4, 34.7 (*C*Me$_3$), 31.6, 30.7, 25.5 (C *Me*$_3$) ppm.

MS (CI$^+$) *m/z*: 934 (20%, M$^+$), 843 (100%, M$^+$−CH$_2$Ph).

IR (Nujol) ν cm^{-1}: 1594, 1556, 1461, 1377, 1301, 1259, 1222, 1206.

EA Calc. for $C_{56}H_{78}N_2O_4Zr$: C, 71.98; H, 8.41; N, 3.00. Found: C, 71.68; H, 8.36; N, 2.95%.

4.4.2. [**L**$_2^2$*Zr*(*CH*$_2$*Ph*)$_2$]

Yield 205 mg, 79%. ^{1}H NMR δ_H (400 MHz, 298 K, C_6D_6) 7.81 (2H, d, $^4J_{HH} = 2$ Hz, Ar–*H*), 7.69 (2H, d, $^4J_{HH} = 2$ Hz, Ar–*H*), 6.97 (4H, d, $^3J_{HH} = 7$ Hz, Ar–*H*), 6.88 (4H, t, $^3J_{HH} = 8$ Hz, Ar–*H*), 6.60 (2H, t, $^3J_{HH} = 7$ Hz,

Ar–*H*), 4.03 (2H, dd, $^2J_{HH} = 8$ Hz, $^3J_{HH} = 3$ Hz, oxazoline CH_2), 3.60 (2H, dd, $^2J_{HH} = 8$ Hz, $^3J_{HH} = 3$ Hz, oxazoline C*H*), 3.16 (2H, m, oxazoline CH_2), 3.03 (2H, d, $^2J_{HH} = 10$ Hz, benzyl CH_2), 2.73 (2H, d, $^2J_{HH} = 10$ Hz, benzyl CH_2), 1.78 (18H, s, ^{t}Bu) 1.35 (2H, m, C*H*Me$_2$), 1.17 (18H, s, ^{t}Bu), 0.18 (6H, d, $^3J_{HH} = 8$ Hz, CH_3), 0.15 (6H, d, $^3J_{HH} = 8$ Hz, CH_3) ppm.

^{13}C{^{1}H} NMR δ_C (100.6 MHz, 298 K, C_6D_6) 169.5, 161.2, 150.9, 141.1, 138.7, 130.0, 128.1, 125.9, 124.2, 119.7 (Ar), 115.5 (*C*=N), 69.8, (*C*H), 68.3 (benzyl *C*H$_2$), 67.1 (oxazoline *C*H$_2$), 36.0, 34.5 (*C*Me$_3$), 31.5, 30.6 (C *Me*$_3$), 30.0 (*C*HMe$_2$), 19.2, 14.8 (CH_3) ppm.

MS (CI$^+$) *m/z*: 905 (20% MH$^+$), 813 (50%, M$^+$−CH$_2$Ph), 723 (30%, M$^+$−2 × CH$_2$Ph).

IR (Nujol) *v* cm^{-1}: 1613, 1580, 1462, 1377, 1260, 1206, 1103, 1018.

EA Calc. for $C_{54}H_{74}N_2O_4Zr$: C, 71.56; H, 8.23; N, 3.09. Found: C, 71.36; H, 8.08; N, 3.12%.

4.4.3. [$L_2^3Zr(CH_2Ph)_2$]

Yield 190 mg, 83%. ^{1}H NMR δ_H (400 MHz, 298 K, C_6D_6) 7.87 (2H, d, $^4J_{HH} = 3$ Hz, Ar–*H*), 7.73 (2H, d, $^4J_{HH} = 3$ Hz, Ar–*H*), 7.04 (6H, m, Ar–*H*), 6.93 (3H, m, Ar–*H*), 6.80 (5H, m, Ar–*H*), 6.70 (6H, m, Ar–*H*), 4.95 (2H, dd, $^2J_{HH} = 9$ Hz, $^3J_{HH} = 4$ Hz, oxazoline CH_2), 3.60 (2H, dd, $^2J_{HH} = 9$ Hz, $^3J_{HH} = 4$ Hz, oxazoline C*H*), 3.46 (2H, dd, $^3J_{HH} = 8$ Hz, $^4J_{HH} = 1$ Hz, oxazoline CH_2), 3.33 (2H, d, $^2J_{HH} = 10$ Hz, benzyl CH_2), 2.90 (2H, d, $^2J_{HH} = 10$ Hz, benzyl CH_2), 2.05 (18H, s, ^{t}Bu) 1.51 (18H, s, ^{t}Bu) ppm.

^{13}C{^{1}H} NMR δ_C (100.6 MHz, 298 K, C_6D_6) 169.6, 161.4, 150.7, 140.5, 140.2, 137.9, 129.6, 129.3, 128.5, 125.7, 124.7, 119.7 (Ar), 115.9 (*C*=N), 74.8, (oxazoline *C*H$_2$), 68.5 (*C*H), 67.8 (benzyl *C*H$_2$), 36.0, 34.5 (*C*Me$_3$), 31.8, 30.7 (C *Me*$_3$) ppm.

MS (CI$^+$) *m/z*: 897 (35%, M$^+$-Ph), 883 (100%, M$^+$−CH$_2$Ph).

IR (Nujol) *v* cm^{-1}: 1610, 1574, 1456, 1377, 1299, 1261, 1222, 1204, 1112, 1026.

EA Calc. for $C_{60}H_{70}N_2O_4Zr$: C, 73.96; H, 7.24; N, 2.87. Found: C, 73.95; H, 7.16; N, 2.83%.

4.5. Zirconium chlorides

4.5.1. [$L_2^1ZrCl_2$]

A Schlenk vessel was charged with (*S*)-H**L**^{1} (362 mg, 1.09 mmol) and NaH (52 mg, 2.18 mmol). THF (20 ml) was added, and the resulting white suspension was stirred under reduced pressure for 15 h. After this time the stirring was ceased and unreacted NaH was allowed to settle. The solution was passed through a filter cannula into a Schlenk vessel charged with $ZrCl_4(THF)_2$ (206 mg, 0.545 mmol) at 0 °C. After stirring for 45 min, the ice bath was removed and the reaction vessel was allowed to warm to ambient temperature. Stirring was continued for 15 h. After this time the solution was filtered, and the filtrate was evaporated in vacuo to yield a pale yellow solid. This material was sublimated at 260 °C, 10^{-6} mmHg, to yield a pale yellow solid. Yield 250 mg, 56%.

^{1}H NMR δ_H (400 MHz, 298 K, C_6D_6) 8.09 (2H, d, $^4J_{HH} = 2$ Hz, Ar–*H*), 7.69 (2H, d, $^4J_{HH} = 2$ Hz, Ar–*H*), 5.54 (2H, dd, $^2J_{HH} = 8$ Hz, $^3J_{HH} = 2$ Hz, CH_2), 4.33 (2H, dd, $^2J_{HH} = 8$ Hz, $^3J_{HH} = 2$ Hz, C*H*), 4.25 (2H, t, $^3J_{HH} = 8$ Hz, CH_2), 1.50 (18H, s, ^{t}Bu) 1.34 (18H, s, ^{t}Bu), 1.12 (18H, s, ^{t}Bu) ppm.

^{13}C{^{1}H} NMR δ_C (100.6 MHz, 298 K, C_6D_6) 173.3, 161.0, 141.4, 138.0, 131.1, 123.8 (Ar), 114.3 (*C*=N), 79.8 (*C*H), 70.2 (*C*H$_2$), 36.2, 35.1, 34.5 (*C*Me$_3$), 31.5, 30.0, 26.4 (C *Me*$_3$) ppm.

MS (CI$^+$) *m/z*: 822 (100%, M$^+$), 785 (70%, M$^+$−Cl), 765 (15%, M$^+$−^{t}Bu).

IR (Nujol) *v* cm^{-1}: 1606, 1556, 1544, 1461, 1378, 1310, 1281, 1259, 1228, 1200.

EA Calc. for $C_{42}H_{64}Cl_2N_2O_4Zr$: C, 61.29; H, 7.84; N, 3.40. Found: C, 61.21; H, 7.87; N, 3.25%.

4.5.2. [$L_2^2ZrCl_2$]

Yield 186 mg, 63%. ^{1}H NMR δ_H (400 MHz, 298 K, C_6D_6) 7.91 (2H, d, $^4J_{HH} = 2$ Hz, Ar–*H*), 7.73 (2H, d, $^4J_{HH} = 2$ Hz, Ar–*H*), 3.95 (2H, dd, $^2J_{HH} = 9$ Hz, $^3J_{HH} = 3$ Hz, CH_2), 3.79 (2H, dd, $^2J_{HH} = 9$ Hz, $^3J_{HH} = 3$ Hz, C*H*) 3.25 (2H, t, $^3J_{HH} = 8$ Hz, oxazoline CH_2), 1.89 (18H, s, ^{t}Bu) 1.73 (2H, m, C*H*Me$_2$) 1.48 (18H, s, ^{t}Bu), 0.85 (6H, d, $^3J_{HH} = 7$ Hz, CH_3), 0.80 (6H, d, $^3J_{HH} = 7$ Hz, CH_3) ppm.

^{13}C{^{1}H} NMR δ_C (100.6 MHz, 298 K, C_6D_6) 173.8, 161.4, 142.0, 140.5, 131.5, 123.5 (Ar), 113.7 (oxazoline C=N), 72.5 (*C*H), 69.9 (*C*HMe$_2$), 67.0 (*C*H$_2$), 35.9, 34.6 (*C*Me$_3$), 31.4, 30.1 (C *Me*$_3$), 19.3, 18.8 (*C*H$_3$) ppm.

MS (CI$^+$) *m/z*: 794 (100%, M$^+$), 759 (70%, M$^+$−Cl).

IR (Nujol) *v* cm^{-1}: 1602, 1458, 1377, 1260, 1024, 798, 721.

EA Calc. for $C_{40}H_{60}Cl_2N_2O_4Zr$: C, 60.43; H, 7.61; N, 3.52. Found: C, 60.19; H, 7.62; N, 3.41%.

4.6. Crystallography

Crystals of Λ-*trans*, *cis*, *cis*-[$L_2^1Zr(CH_2Ph)_2$] were coated in an inert oil prior to transfer to a cold nitrogen gas stream on Bruker-AXS SMART three circle area detector diffractometer system equipped with Mo Kα radiation ($\lambda = 0.71073$ Å). Data were collected with narrow (0.3° in ω) frame exposures. Intensities were corrected semi-empirically for absorption, based on symmetry-equivalent and repeated reflections (SADABS). Structures were solved by direct methods (SHELXS [23]) with additional light atoms found by Fourier methods. All H atoms were constrained with a riding model; *U*(H) was set at 1.2 (1.5 for methyl groups) times U_{eq} for the parent atom. Programs used were Bruker AXS SMART (control), SAINT (integration) and SHELXTL [23] for structure solution, refinement, and molecular graphics. Yellow block, $C_{56}H_{78}N_2O_4Zr$, Monoclinic, P2(1), $a = 10.7948(7)$, $b = 18.3340(13)$, $c = 13.4520(9)$ Å,

$\beta = 92.1260(10)°$, $V = 2660.5(3)$ Å^3, $Z = 2$, $\mu = 0.250$ mm^{-1}, total reflections = 14069, independent reflections = 7711 [$R^{int} = 0.0.0817$], R_1, wR_2[I > 2(*I*)] 0.0864, 0.2002.

4.7. DFT calculations

All DFT calculations employed the Amsterdam density functional (ADF) program version 2005.01. Geometries were optimised in the gas phase at the local density approximation level using a triple-ζ + p STO basis set on Zr (ADF basis TZP), double-ζ + polarisation bases on the ligand donor atoms (ADF basis DZP) and double-ζ bases on all remaining atoms (ADF basis DZ). Single-point energies were then computed with the PW91 gradient corrected functional. A 3d frozen core was used for Zr and 1s frozen cores for O, N and C. Default convergence criteria were employed throughout.

5. Supplementary material

Crystallographic data for the structural analysis of [$\mathbf{L}^1_2$Zr(CH$_2$Ph)$_2$] have been deposited with the Cambridge Crystallographic Data Centre, CCDC No. 286257. Copies of this information may be obtained free of charge from The Director, CCDC, 12 Union Road, Cambridge CB2 1EZ, UK (fax: +44 1223 336 033; e-mail: deposit@ccdc.cam.ac.uk or www: http://www.ccdc.cam.ac.uk).

Acknowledgements

P.S. thanks the University of Warwick for a Postgraduate Research Fellowship (to I.W.) and EPSRC for support.

References

[1] A.P. Smirnoff, Helv. Chim. Acta 3 (1920) 177.
[2] A. Werner, A.Z. Vilmos, Allorg. Allg. Chem. 21 (1989) 145.
[3] U. Knof, A. von Zelewsky, Angew. Chem., Int. Ed. Engl. 38 (1999) 302.
[4] A. von Zelewsky, O. Mamula, J. Chem. Soc., Dalton Trans. (2000) 219.
[5] H. Brunner, Angew. Chem., Int. Ed. Engl. 38 (1999) 1195.
[6] K. Muñiz, C. Bolm, Chem. Eur. J. 6 (2000) 2309.
[7] (a) H. Brunner, Eur. J. Inorg. Chem. (2001) 905;
(b) C. Ganter, Chem. Soc. Rev. 32 (2003) 130;
(c) J.W. Faller, A.R. Lavoie, New. J. Chem. 27 (2003) 899.
[8] P.D. Knight, P. Scott, Coord. Chem. Rev. 243 (2003) 125.
[9] E.J. Crust, I.J. Munslow, C. Morton, P. Scott, J. Chem. Soc., Dalton Trans. (2004) 2257.
[10] E.J. Crust, A.J. Clarke, R.J. Deeth, C. Morton, P. Scott, J. Chem. Soc., Dalton Trans. (2004) 4050.
[11] I.J. Munslow, A.R. Wade, R.J. Deeth, P. Scott, Chem. Commun. (2004) 2596.
[12] I.J. Munslow, A.J. Clarke, R.J. Deeth, I. Westmoreland, P. Scott, Chem. Commun. (2002) 1868.
[13] A.J. Davenport, D.L. Davies, J. Fawcett, D.R. Russell, Dalton Trans. (2004) 1481.
[14] P.G. Cozzi, C. Floriani, A. Chiesi-Villa, C. Rizzoli, Inorg. Chem. 34 (1995) 2921;
P.G. Cozzi, E. Gallo, C. Floriani, A. Chiesi-Villa, C. Rizzoli, Organometallics 14 (1995) 4994;
R.K.J. Bott, M. Hammond, P.N. Horton, S.J. Lancaster, M. Bochmann, P. Scott, Dalton Trans. 22 (2005) 3611.
[15] M.J. Miller, P.G. Mattingley, M.A. Morrison, J.F. Korwin, J. Am. Chem. Soc. 102 (1980) 7026.
[16] (a) H. Vorbruggen, K. Krolikiewicz, Tetrahedron Lett. 22 (1981) 4471;
(b) H. Vorbruggen, K. Krolikiewicz, Tetrahedron 49 (1993) 9353.
[17] A. Scheurer, P. Mosset, W. Bauer, R.W. Saalfrank, Eur. J. Org. Chem. 0 (2001) 3067.
[18] S. Rajaram, M.S. Sigman, Org. Lett. 4 (2002) 3399.
[19] P.R. Woodman, P.B. Hitchcock, P. Scott, Chem. Commun. (1996) 2735.
[20] P.D. Knight, P.N. O'Shaughnessy, I.J. Munslow, B.S. Kimberley, P. Scott, J. Organomet. Chem. 683 (2003) 103.
[21] G. Milano, L. Cavallo, G. Guerra, J. Am. Chem. Soc. 124 (2002) 13368.
[22] For a discussion of this concept, see M. Asakawa, G. Brancato, M. Fanti, D.A. Leigh, T. Shimizu, A.M.Z. Slawin, J.K.Y. Wong, F. Zerbetto, S.W. Zhang, J. Amer. Chem. Soc. 124 (2002) 2939.
[23] G.M. Sheldrick, SHELXTL Ver 5.1, Bruker Analytical X-ray Systems, 1997.